Acta of Bioengineering and Biomechanics
Vol. 16, No. 3, 2014

Original paper
DOI: 10.5277/abb140301

Gradient composite materials for artificial intervertebral discs

KATARZYNA MIGACZ[1], JAN CHŁOPEK[1]*, ANNA MORAWSKA-CHOCHÓŁ[1], MACIEJ AMBROZIAK[2]

[1] AGH University of Science and Technology, Faculty of Materials Science and Ceramics, Department of Biomaterials, Kraków, Poland.
[2] Cathedral and Clinic of Orthopaedics and Traumatology of the Motor System at Medical University of Warsaw, Warsaw, Poland.

Composites with the gradient of Young's modulus constitute a new group of biomimetic materials which affect the proper distribution of stresses between the implant and the bone. The aim of this article was to examine the mechanical properties of gradient materials based on carbon fibre-polysulfone composite, and to compare them to the properties of a natural intervertebral disc. Gradient properties were provided by different orientation or volume fraction of carbon fibres in particular layers of composites. The results obtained during *in vitro* tests displayed a good durability of the gradient materials put under long-term static load. However, the configuration based on a change in the volume fraction of the fibres seems more advantageous than the one based on a change of the fibres' orientation. The materials under study were designed to replace the intervertebral disc. The effect of Young's modulus of the material layers on the stress distribution between the tissue and the implant was analyzed and the biomimetic character of the gradient composites was stated. Unlike gradient materials, the pure polysulfone and the non-gradient composite resulted in the stress concentration in the region of nucleus pulposus, which is highly disadvantageous and does not occur in the stress distribution of natural intervertebral discs.

Key words: *composite, gradient material, intervertebral disc replacement*

1. Introduction

The interpenetrating system of liquid and solid substances and changes in the compactness of the bone microstructure create a natural density gradient of the bone tissue [1]. A compact cortical bone smoothly passing to porous spongy bone tissue forms the porosity gradient, which is one of the major causes of the differentiation of mechanical properties. The constant remodeling of the bone create the resorption rate gradient which is essential for the regeneration of the degenerated tissue. The permanent remodeling and adaptation of bone structures to the outside stress and deformation conditions determine the formation of Young's modulus gradient [2].

The spine consists of 24 semirigid presacral vertebrae that are separated by relatively flexible discs. The largest avascular structure in the human body, the intervertebral disc acts as a flexible spacer between adjacent vertebrae and carries significant compressive loads resulting from gravitational and muscular forces. The intervertebral disc consists of an outer annulus fibrosus, which surrounds the inner nucleus pulposus. Under compression the nucleus loses water over time. The literature [3] shows that under *in vitro* conditions the annulus and nucleus can lose, respectively, up to 15% and 10% of their free water in the period of 4 hours. Cyclic compression loading can further increase this loss and consequently decrease the disc's height, which is partly responsible for the well-known diurnal changes in standing height [4].

The development of gradient materials can be another step to create biomaterials endowed with the biomimetic construction comparable to the structure of natural tissue. Adjusting Young's modulus to the natural bone tissue assures such stress and deformation distributions which are natural in physiological

* Corresponding author: Jan Chłopek, AGH University of Science and Technology, Faculty of Materials Science and Ceramics, Department of Biomaterials, al. Mickiewicza 30 30-059 Krakow, Poland, phone number: 126172503, e-mail: chlopek@agh.edu.pl
Received: February 12th, 2014
Accepted for publication: March 12th, 2014

working conditions of the bone. Thus the fourth generation biomaterials are the composites whose chemical and phase compositions are close to those of the bone; they are also gradient materials which cause neither the excessive overload nor the under-loading in the surrounding natural structures at the implant–tissue interface. That is why, composite gradient materials should be included in the evolution of bone surgery materials, as presented by Murugan and Ramakrishna in the form of a scheme [5], (Fig. 1). Gradient composites can be used in guided bone regeneration techniques (GBR), because their gradient structure, especially the gradients of porosity, resorption rate and Young's modulus, can facilitate these processes. In composite materials, these gradients can be obtained through layered structures. The Young's modulus gradient seems to be especially important for the proper distribution of the bone-implant stresses.

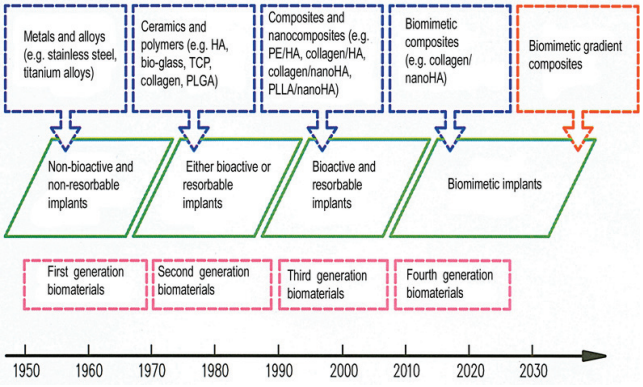

Fig. 1. Evolution of the materials applied in bone surgery [5]

According to the theory of composites, the greatest potential for achieving Young's modulus gradient is applying different volume fractions or orientation of fibres in composite. The aim of this article was to examine the mechanical properties of different gradient materials based on carbon fibre-polysulfone composite and to compare them to the properties of a natural intervertebral disc.

2. Materials and methods

Long carbon fibres produced by Torayca were used to obtain the composite (Young's modulus of 230 GPa, deformation 1.5%, density 1.76 g/cm^3 and the tensile strength of 3530 MPa); The biocompatibility of fibres was verified and documented in work [6]. As the matrix, pure polysulfone was applied, which is proved to be resistant to the effect of acid, base and salt solutions. Polysulfone is very popular for medical applications, as it is inert in the biological environment and compatible with blood and body fluids [7]. The polysulfone used in this work was characterized by the molecular weight of 22000, the melting point 343 °C, the strain to failure 2.8%, and the tensile strength 72.8 MPa.

The methodology of obtaining composites with a gradient lay-out of layers was developed to conduct experimental tests. The gradient was created using two techniques: changing the volume fraction of fibres or changing their orientation (Fig. 2). The prepregs differing in the fibres' volume fractions were used to create the volume fraction gradient. The prepregs with the carbon fibre content of volume fraction $V_f = 0.30$ but with their different orientation were applied to obtain the gradient of the fibre orientation change. The procedure to make samples was as follows. First, carbon fibres 1D were wound round the drum, impregnated with PSU solution and thoroughly dried. Single layers (10 × 10 mm) were cut out with a blanking die according to the designed values of the fibre orientation angle (Figs. 2 and 3). Then the cut out elements were piled in 5 layers, each of them 2 mm thick. The volume fraction and the orientation of fibres in each layer were precisely defined. For the non-gradient composite all the layers had the same fibre orientation and the volume fraction of fibre was 40%. Next, the materials were put into forms and heated in the oven at 240 °C for 30 min. After that they were compacted in high temperature under 5 MPa in a hydraulic press. The final samples were of a cubic shape measuring 10 mm × 10 mm × 10 mm. The markings of particular samples corresponding to different volume/orientation of carbon fibres in PSU are presented in Table 1.

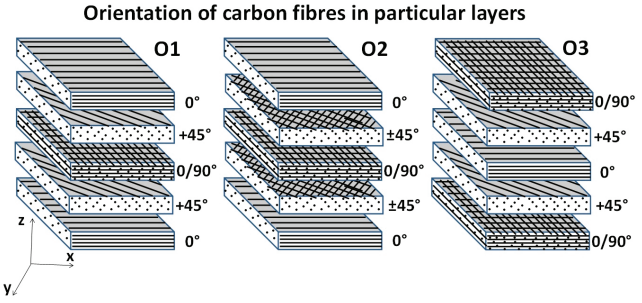

Fig. 2. Orientation of carbon fibres in particular layers

The Young's modulus for samples treated as a whole was determined by a universal testing machine Zwick 1435, with the measuring range up to 5000 N. Moreover, Young's modulus of each layer of the gradient composites was determined – using the MTS 858

MiniBionix (the measuring range up to 15000 N) equipped with the ME 46-350 Messphysik video-extensometer. The extensometer was applied to measure the sample's deformation. A video camera recorded the size changes in each layer of the sample, with the accuracy up to 0.02 mm. The force and time of the measurement were also recorded.

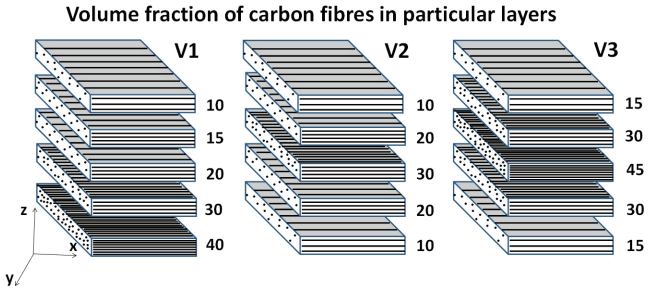

Fig. 3. Volume fraction of carbon fibres in particular layers

Table 1. Gradient packing of particular layers in obtained composites

Designation of samples	Orientation of carbon fibres in particular layers				
O1	0	+45	0/90	+45	0
O2	0	±45	0/90	±45	0
O3	0/90	+45	0	+45	0/90
	Volume fraction of carbon fibres in particular layers				
V1	10	15	20	30	40
V2	10	20	30	20	10
V3	15	30	45	30	15

In order to determine the bonding force at the fibre–matrix interface (ILSS – Interlaminar Shear Strength), the shearing tests were performed with the short beam method using the Tira–Test 2300 testing machine (the measuring range up to 100 kN, according to the standard PN-EN ISO 14130:1997) [8]. The samples with rectangular cross-section were placed on two supports and the force was applied until they bent, similarly to the three point bending test. The interlayer cutting procedure was applied to achieve the effect of damage; the ratio of the width and the thickness of the profile was 5 $h \pm 0.3$ mm (h – the mean thickness of a sample). It develops with the increase of the shearing stress level against the bending stress in the sample. During the test the force F was noted.

The modulus of interlayer cutting σ_{ILSS} was calculated using the following dependence

$$\sigma_{\mathrm{ILSS}} = \frac{3}{4} \cdot \frac{F}{b \cdot h} \tag{1}$$

where F – maximum force during destruction of the sample [N],

b – width of the sample [mm],

h – thickness of the sample [mm].

The fatigue tests were performed using the MTS 810 testing machine, with the assumption of a constant asymmetry coefficient of the cycle $R = 2.5$ for compression. The measurements were taken during the axial compression test. With the assumed stress, the level of displacement of the samples was examined.

Designing a simplified FEM (Finite Element Method) model of the C6–C7 level segment made it possible to verify if Young's modulus of the analysed gradient composites meets the biomimetic criteria of mechanical properties. Gradient composites, PSU-CF1D and PSU were used for intervertebral disc implants in the models. The Young's modulus values of all given elements of the spine segment and the materials studied, as well as anisotropy of their mechanical properties, were included in the model. The spine segment was modeled as an orthotropic material (like spongy bone tissue), intervertebral disc as an orthotropic material, too, while nucleus pulposus as an isotropic material [9]. The assumed implant dimensions (of the vertebra C6 and C7, the fibrous disc and the nucleus pulposus) were the same as those of the intervertebral disc from papers [10], [11]. The implant's height was $h = 6.25$ mm and its width was $w = 22.75$ mm. The dimensions of vertebra C6 and C7 were assumed as 12 mm and 13 mm, respectively [8], [12]. In the spine segment designed, the physiological force was used ($P = 200$ N, according to papers [13], [14]). Next, a numerical solution was obtained in the form of stress distributions in three dimensions. NEiNastran for Windows software and tetra-type elements were used.

3. Results

The elaborated test results of Young's modulus for the samples obtained are collected in Table 2 and compared to the literature data for different types of bone tissue [12]. There are values of Young's modulus both for particular layers of composites (marked as E_1–E_5) and for whole composite samples (marked as E_c). The obtained values of Young's modulus for all the gradient composites are within the range of the properties of the spongy bone, the vertebral arch, the annulus fibrosus of the intervertebral disc and the end-plate [4]. On the basis of this data, it is possible to determine the adjustment of the materials with respect to Young's modulus values and the minimization of over-rigidness risk, when these materials are used in the human spine.

Table 2. List of Young's modulus values for whole composite samples (E_c) and for each layer (E_1–E_5) in "x" direction (regarding Figs. 2, 3)

Material	E_c [GPa]	E_1 [GPa]	E_2 [GPa]	E_3 [GPa]	E_4 [GPa]	E_5 [GPa]
V1	0.69 ± 0.10	0.35 ± 0.04	0.59 ± 0.05	1.49 ± 0.15	2.11 ± 0.08	0.63 ± 0.10
V2	0.76 ± 0.02	0.78 ± 0.12	2.91 ± 0.45	0.55 ± 0.04	1.69 ± 0.21	1.14 ± 0.16
V3*	0.52 ± 0.02	0.81 ± 0.07	2.57 ± 0.09	0.77 ± 0.06	1.64 ± 0.14	1.82 ± 0.21
O1 **	0.60 ± 0.05	1.92 ± 0.09	2.44 ± 0.5	0.27 ± 0.03	2.19 ± 0.09	1.27 ± 0.03
O2	1.15 ± 0.14	1.20 ± 0.20	1.00 ± 0.05	0.71 ± 0.07	1.11 ± 0.03	1.13 ± 0.04
O3	0.55 ± 0.06	0.75 ± 0.07	1.42 ± 0.15	0.41 ± 0.03	2.27 ± 0.35	0.34 ± 0.04
Pure PSU	1.05 ± 0.15	–	–	–	–	–
Spongy bone [12]	0.05–0.1					
Vertebral arch [12]	0.5–1.5					
End-plate [12]	0.5–1.0					
Annulus fibrosus [12]	0.25–0.9					

* Composite composed of layers with the proper volume fractions of the fibres.
** Composite composed of layers with the proper orientation angle of the fibres.

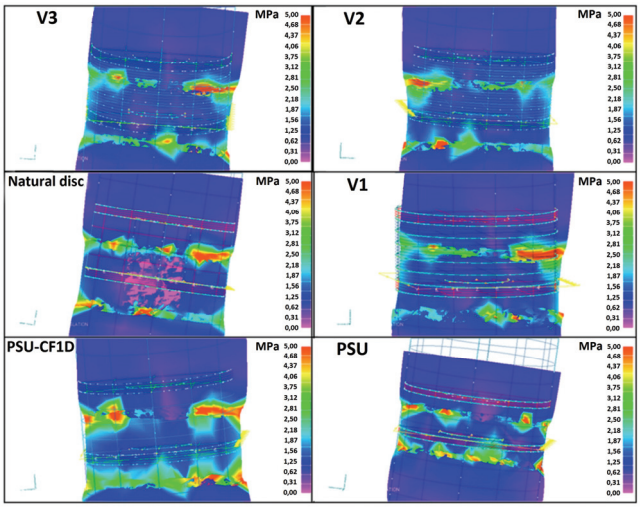

Fig. 4. Comparison of the stress distributions of the composite with the fibre volume fraction gradient, the pure PSU and the non-gradient composite PSU–CF 1D with a simplified natural spine C6–C7 segment

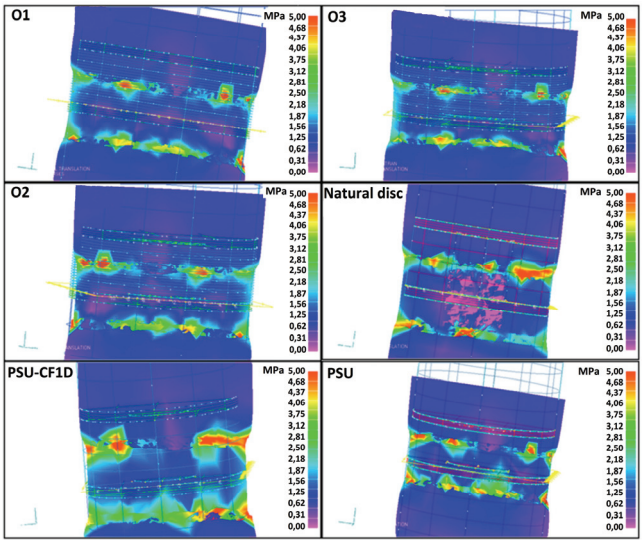

Fig. 5. Comparison of the stress-deformation characteristics of the composites with the fibre orientation gradient, the pure PSU and the non-gradient composite CF 1D with a simplified natural spine C6–C7 segment.

In order to verify if Young's modulus of gradient composites meets the biomimetic criteria of the mechanical properties of C6–C7 segment, FEM was used. Figure 4 shows the comparison of stress distribution in the natural spine segment and in the materials with the gradient obtained by changing the fibers' volume fraction, the non-gradient composite (PSU–CF1D) and the pure polysulfone. All the composites with the gradient introduced by changing the fibers' volume fraction do not distort the stress distribution in the C6–C7 spine segment. The pure PSU and the non-gradient composite PSU–CF 1D cause a distortion in the stress distribution, which can result in the occurrence of local over-loading as well as under-loading of the spine segment analysed.

Figure 5 presents the stress distributions of the materials with the fibre orientation gradient, the pure PSU and the non-gradient composite PSU–CF 1D in comparison to the natural C6–C7 segment. The comparison of the stress distributions of the gradient composites with those of the intervertebral disc shows a biomimetic character of the gradient materials, whose Young's modulus is well adjusted and does not distort the stress distribution of the cervical spine segment C6–C7. The non-gradient composite PSU–CF 1D is not biomimetic and causes a change in the stress distribution by concentrating stresses in the central part of the implant, which is not observed in the natural segment. The pure polysulfone modeled as an implant also causes a disadvantageous stress concentration in the area of nucleus pulposus.

The influence of the fibres' volume fraction on average stress values for each area of the C6–C7 seg-

ment is shown in Fig. 6. The results are described in comparison to the natural intervertebral disc. The diagram shows the stress values of a non-gradient composite (PSU–CF1D) and pure polysulfone (PSU), too. The stress values of the composites V1, V2, V3 are the closest to the respective values of the natural intervertebral disc. The best matching was observed for the composites V1. The non-gradient composite causes a non-match in the stress values for the whole area of C6–C7. There is also a distortion of the stress values caused by the pure polysulfone implant.

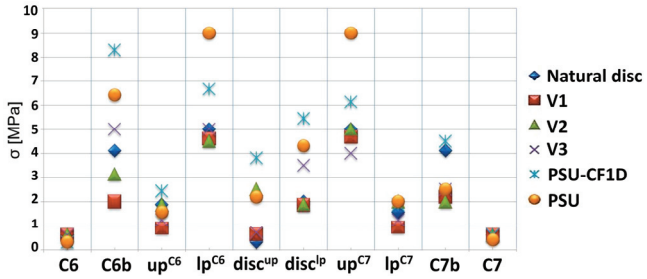

Fig. 6. Compressive stress values for each layer of the composite with the gradient introduced by changing the fibers' volume fraction, compared to the natural spine segment. Assumed markings: C6 vertebra (**C6**); C6 vertebra at the border with end-plate (**C6b**); end-plate at the level C6 – upper part (**up**^{C6}); end-plate at the level C6 – lower part (**lp**^{C6}); intervertebral disc – upper part (**disc**^{up}); intervertebral disc – lower part (**disc**^{lp}); end-plate at the level C7 – upper part (**up**^{C7}); end-plate at the level C7 – lower part (**lp**^{C7}); C7 vertebra at the border with end-plate (**C7b**); C7 vertebra (**C7**)

Figure 7 presents respective average stress values for composites with different fibres' orientation. The composites with the best suited systems are the gradient materials: O1, O2, O3. The composite PSU–CF1D and the pure PSU distort the stress values of the natural disc.

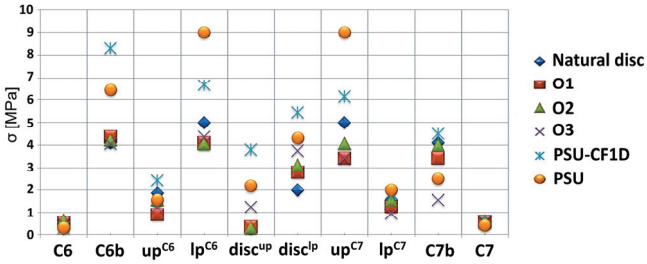

Fig. 7. Compressive stress results for each layer of the composite with the gradient introduced by changing the fibre orientation, compared to the natural spine segment. Assumed markings: C6 vertebra (**C6**); C6 vertebra at the border with end-plate (**C6b**); end-plate at the level C6 – upper part (**up**^{C6}); end-plate at the level C6 – lower part (**lp**^{C6}); intervertebral disc – upper part (**disc**^{up}); intervertebral disc – lower part (**disc**^{lp}); end-plate at the level C7 – upper part (**up**^{C7}); end-plate at the level C7 – lower part (**lp**^{C7}); C7 vertebra at the border with end-plate (**C7b**); C7 vertebra (**C7**)

Figure 8 presents exemplary results of the compressive force tests conducted on the materials with the gradient obtained by a change of the fibers' volume fractions before and after their incubation under *in vitro* conditions (84 days incubation in Ringer's fluid at 37 °C under the static load of P = 1200 N). For the initial samples with the axial compression up to 5000 N, the value of E was E = 0.53±0.03 GPa, while after *in vitro* incubation under a constant load, Young's modulus value equalled E = 0.50±0.04. The decrease in the modulus value by 5.7% is within the range of measuring error. The Young's modulus values of all the samples tested (five samples in each series) are in the range of those of the annulus fibrosus of the intervertebral disc, which has been proved in the paper.

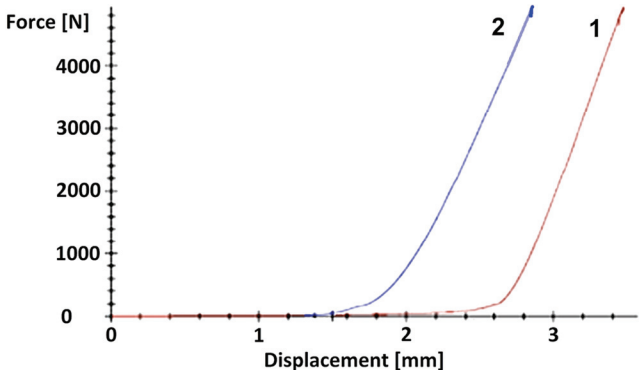

Fig. 8. Comparison stress deformation characteristics of material V1: initial material (line 1) and after 84 days of *in vitro* incubation (line 2)

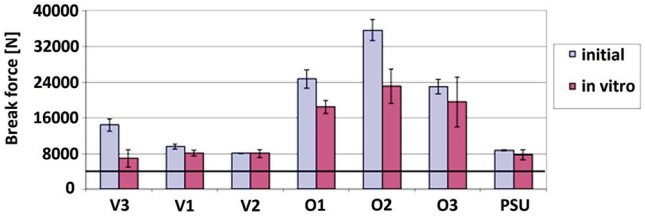

Fig. 9. Comparison of the ultimate force values for the initial materials and those after incubation under a time-constant load

Axial compression tests till failure of the materials were also conducted for all gradient composites and pure PSU. The aim of the tests was to determine the effect of *in vitro* incubation on the durability of materials under a time-constant load. The test results compared to the initial sample values are compiled in Fig. 9. After 84 days of incubation under constant-load conditions, a decrease of the ultimate force was observed in each sample. For the materials V1 and V2 and the pure polysulfone the ultimate force drop was the low-

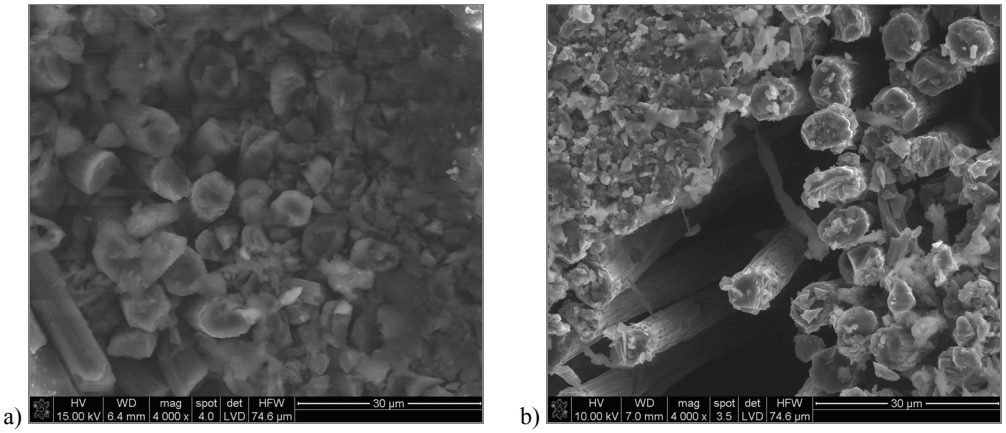

Fig. 10. Material O1: (a) initial sample, (b) sample after failure in the static test

est, within the range of measuring error. The cross-sections of all the samples were the same. The biggest difference between the "dry" and the *in vitro* ultimate forces was 51.6% for samples V3. In the case of the material O2, the difference was 35.3%. For the composites O1, a 25.6% drop of the ultimate force was recorded. The weakening of the ultimate force after the incubation of the materials (under the constant load, for 84 days) proves facilitated penetration of the fluid and the weakening of the phase boundaries between the fibre and the polymer matrix. Figure 10 shows an example microphotograph of the composite O1 – at the initial stage and after the failure. It shows fractures in the polysulfone matrix and locally, pulling the fibres out of the matrix.

All the gradient composites possess a sufficient interlaminar shear strength (ILSS), as compared to the one of the intervertebral disc. The highest σ_{ILSS} values were exhibited by the material V3, and the lowest one – by the material O3 (Table 3). The material O3 may seem doubtful, as its σ_{ILSS} value is not much higher than the stress values available in the literature data [15], [16]. The σ_{ILSS} values of all the other materials are over twice as high as the stress values for the human intervertebral disc.

Table 3. Interlaminar shear strength of the materials tested compared to the intervertebral disc

	σ_{ILSS} [MPa]
O1	4.51±1.76
O2	3.71±1.08
O3	1.79±0.31
V1	4.80±1.48
V2	7.47±1.10
V3	8.92±1.85
Intervertebral disc [27]	1.67
Intervertebral disc [28]	0.4–1.0

The shearing strength of the implant–bone tissue interface for the polysulfone composite reinforced with carbon fibre, examined by the push-up test [17], is situated within the range of 1.5–1.8 MPa. The comparison of this value to the σ_{ILSS} value of the intervertebral disc (Table 3) shows that they are similar, which proves the possibility of creating a good connection between the polysulfone composite reinforced with carbon fibre and the bone tissue. Although the mere shear strength values are not very high as compared to the other composites, they are sufficient when considering the literature data on the intervertebral disc and the interlaminar shear strength at the implant–bone tissue interface (during the incubation time, under *in vitro* conditions).

On the basis of the model tests with the use of FEM, the statistic test results and the results obtained from the *in vitro* incubation under time-constant load, the material V1 was selected for the fatigue tests. Its Young's modulus gradient is the best match for the annulus fibrosus of the intervertebral disc and it possesses the best stress-strain characteristics. The change of the sample lateral dimensions by the value of $\Delta W = 0.5$ mm was assumed as its failure criterion. The idea behind it was that the fatigue failure process can also take place as a result of microfractures created during the production of composites [15]. The tests were initiated by applying the maximum value of the compression stress $S_{max} = 100$ MPa, and the lower compression stress level was assumed to be $S_{min} = 40$ MPa, according to the assumed asymmetry coefficient of the cycle. The amplitude S_a was variable – from 30 to 25.8 MPa. The assumed frequency was $f = 30$ Hz. During the measurements a failure propagation was observed due to a characteristic "crater", which always occurred in the same two layers of the material with the highest fibre content (30% and 40%). This phenomenon is presented in Figs. 11 and 12.

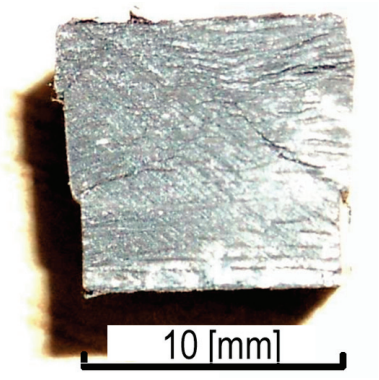

Fig. 11. Failure mechanism for an exemplary sample V1

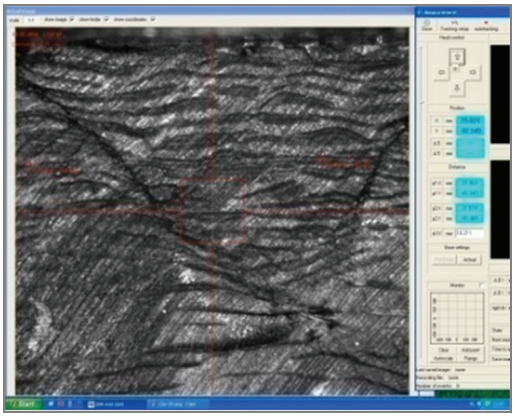

Fig. 12. Failure mechanism for an exemplary sample during the test

The fracture propagated from the layer with the 40% fibre content towards the composite's central layers. Still it should be noted that a majority of the samples exceeded the assumed failure criterion (ΔW = 0.5 mm) without losing their load capacity. On the basis of the measurements performed, the mean stress value S_m was determined according to the following dependence

$$S_m = \frac{|S_{\max} + S_{\min}|}{2} \quad \text{[MPa]}. \tag{2}$$

Next, the dependence of the mean stress as a function of the failure cycle number N_f was drawn, which the literature describes as the Wöhler curve [16]. After the measurements, the Wöhler curve was drawn for the samples tested, which is illustrated in Fig. 13. On the basis of the analysis of the measurement results with the use of the papers, it was proved that the value $S_m = 48.73 \pm 0.07$ is the border for the fatigue strength for material V1.

The standard deviation from this value was determined for the assumed binominal distribution.

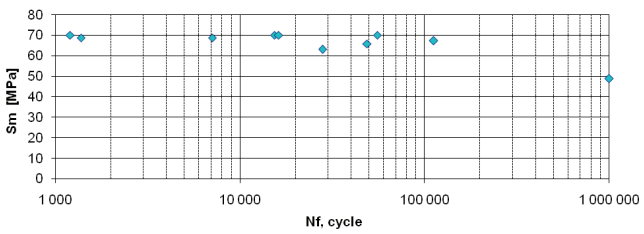

Fig. 13. Mean stress dependence as a function of the number of cycles

4. Discussion

Taking into consideration the implant's activity in natural physiological conditions, the combination between the bone tissue and the gradient material is much more advantageous than the one with the non-gradient composite. The gradient material matches the natural system of the bone tissue and it does not cause the undesirable presence of stress concentrations, which has been proved in the previous tests. All the gradient composites display a biomimetic matching with the stress distribution of the natural intervertebral disc. They do not create stress concentration areas, unlike the pure polysulfone and the non-gradient composite, which was studied both in this work and in other authors' papers [18]–[20]. The composites with the best gradient systems are V1 and V2, i.e., composites with the gradient introduced by changing the fibers' volume fraction. Among the composites with the gradient introduced by diversifying the fibre orientation, the best systems are O1 and O3. The gradient layer systems of V3 and O2 also have a good biomimetic matching, yet they cause a the slight stress level increase in the central area of the lower endplate (beside the nucleus pulposus).

The measurements of the axial compressive strength and the accompanying displacement made it possible to obtain the deformation characteristics of the gradient materials examined, which were next compared to the characteristic stress and deformation values of the natural elements of human spine (Table 4). The maximum displacements for discs are within the range of 1–2 mm; the displacements of all the gradients are in the same range. The deformation values of the natural annulus fibrosus of the lumbar spine are contained within a wide range, depending on the stress. The deformations for all the materials tested are within the same range, too. Table 4 includes the ultimate force values for the particular materials. Since the forces affecting intervertebral discs are at least ten times weaker than those affecting the composite, all the gradient materials can be safely applied because of

Table 4. Comparison of the results of mechanical property tests by the dry method to the literature data

Material	σ_s [MPa]	ε [%]	F [N]	Δl [mm]
V1	119.04 ± 13.88	13.33 ± 4.16	9770.0 ± 390.0	1.38 ± 0.42
V2	153.96 ± 12.34	15.11 ± 3.12	14540 ± 1232.9	0.69 ± 0.09
V3	303.99 ± 42.01	12.32 ± 1.98	14420.0 ± 1321.0	1.23 ± 0.14
O1	247.02 ± 20.10	17.79 ± 3.45	24700 ± 2112.3	0.85 ± 0.08
O2	338.29 ± 21.01	16.87 ± 2.15	35680 ± 2310.2	1.70 ± 0.19
O3	262.06 ± 18.05	30.95 ± 4.16	23010 ± 1650.0	1.77 ± 0.23
PSU	103.72 ± 9.87	7.5 ± 0.67	11500 ± 98.56	0.80 ± 0.03
PSU-CF1D	82.50 ± 4.85	3.1 ± 0.09	3041.48 ± 2.80	1.15 ± 0.12
Intervertebral disc in cervical spine, level [17]				
C2–C3	3.93 ± 2.31		602	1.4
C3–C4	4.26 ± 3.84		683	1.5
C4–C5	4.46 ± 3.00		777	1.6
C5–C6	3.33 ± 2.57		664	1.6
C6–C7	2.67 ± 1.88		673	1.7
C7–T1	3.37 ± 2.09		910	1.6
Max. disc relocation [2]				1–2
Annulus fibrosus deformation [11]		5–25		

their high compressive strength values. A very important factor which significantly weakens the material's properties is the presence of human physiological fluids. Moreover, the material replacing the natural disc is exposed to the pressure force coming both from the head and the preceding spine segments [8], [12]. That is why the gradient materials tested were exposed to the effect of the static force P = 1200 N and were placed in Ringer's fluid for the period of about 84 days.

For the initial samples, close connections between the fibres in the polysulfone matrix were observed. After the failure, the separation of the fibres from the matrix was noted together with the delamination of the composite. These phenomena were caused by the fracture increase inhibition mechanism; the fractures initiated in the matrix do not spread out catastrophically in the whole volume of the material but they stop at the point of the fibres. The failure of the matrix can be seen, while the carbon fibres maintain their structure. After the failure of the outer layer of polymer matrix, the Ringer's fluid can more easily penetrate inside the composite, causing its delamination, which significantly affects the decrease of its mechanical properties. The drop of the ultimate force value – caused by the long-term loading in the aggressive biological environment – probably resulted from the reactions happening at the fibre–matrix interface. It took place due to the penetration of Ringer's fluid inside the material. This process could have been facilitated by local inhomogeneities caused by non-uniform distribution of fibres, which might occur during the technological process of sample production. The highest biostability was stated for materials V1, V2 and O3 – the observed changes are within the range of measuring error. The material V3 is not suitable for a long-term use, as the drop of its ultimate force after the incubation under time-constant loading is too big (over 50%). Assuming the unsurpassable border of the force which the material must bear to be P = 4000 N, the value 6975.00 ± 1944.54 N is too low for the material to be safely applied as a spine implant. The value of Young' modulus for the annulus fibrosus of intervertebral disc equals 0.25–0.9 GPa, the one for the end-plate is 0.5–1 GPa, and that for the vertebral arch – 0.5–1.5 GPa [4]. When comparing these values to Young's modulus of the composites, it is clear that the materials tested meet the criterion of Young's modulus matching with the annulus fibrosus of intervertebral disc. Additionally, it is sure that the composites maintain their full strength properties in the range up to 5000 N. The materials with the gradient introduced by the fibre orientation are characterized by the biggest strength drops after the 84-day incubation in Ringer's fluid, which can result from the strong anisotropy of their mechanical properties in all directions. The composites with the fibres' volume fraction gradient, being orthotropic materials, do not exhibit such a high compression strength, yet their biostability is much better and thus they are best adjusted to the biomimetics of natural intervertebral discs. Besides, due to the course of their deformation characteristics (similar to the natural fibrous ring), the probability of a catastrophic loss of their load capacity is low, similarly to that of the

human disc. In order to determine the bonding force at the fibre–matrix interface, the shearing tests were performed with the short beam method.

The results of the *in vitro* tests performed with a time-constant load, obtained for materials V1, V2 and O3 prove a good strength of the latter during a long-term, static load under *in vitro* conditions. These results prove advantages of the gradient system introduced by changing fibres' volume fraction. The remaining materials exhibit a significant change in their anisotropy degree, pointing to the degradation processes occurring. It can result from the facilitated fluid penetration caused by the insufficient wettability of the fibres through the polysulfone matrix.

On the basis of the analysis performed, it was proved that the value $S_m = 48.73 \pm 0.07$ is the fatigue strength border for material V1. For the natural intervertebral disc, the values of operating compression forces (corresponding to the trunk's load above the given segment) are within the range of 222–444 N, according to [21], and 300–600 N, according to [22]. The discrepancies in the literature are significant, yet the most important conclusion is the fact that the physiological pressure forces operating on intervertebral discs from the side of the trunk do not exceed 1000 N. In paper [23], the highest normal stress value for the annulus fibrosus of intervertebral disc in the vertical direction equals 0.85 MPa, and that for the nucleus pulposus is 1.61 MPa. Even with the assumption that the border strength value for the lumbar spine equals 39.24 MPa (calculated according to paper [24]), there is still a large margin for the thesis that the material V1 exhibits the required fatigue strength parameters. It is worth mentioning that the failure criterion, which is the dimension change of $\Delta W = 0.5$ mm, was very strictly selected and only a part of the samples tested merely exceeded the assumed failure border, without losing their load capacity. On the basis of the tests conducted, it was proved that the material discussed can be applied as intervertebral disc implants with the satisfactory parameters of its fatigue strength.

Summing up, the elaborated gradient composites meet the biomechanical requirements for intervertebral discs. Their mechanical and biomechanical properties are similar to the characteristics of natural discs. These features distinguish the gradient composites from the other artificial discs, such as the ones based on metallic materials with the polymer insert [25], [26] or on polymer composites without gradient properties [18]–[20].

5. Conclusions

- Having compared the characteristics of non-gradient composites and the pure polymer to the properties of the gradient materials, it is clear that the gradient composites have obvious advantages. The combination of the bone tissue and the gradient material promotes better implant's functioning in the natural physiological conditions of a human organism. The pure isotropic polysulfone and the non-gradient composite designed to replace the intervertebral disc create the stress concentration areas at the point of the nucleus pulposus. It is a very disadvantageous phenomenon as far as the stress distribution is concerned, which does not occur in the natural stress pattern for intervertebral discs.
- The obtained Young's modulus values for all the gradient composites are within the property range of the spongy bone, the vertebral arch, the annulus fibrosus of intervertebral disc and the end-plate [4]. The biomimetic character of the gradient materials was proved by comparing the direct effect of Young's modulus of the particular material layers on the stress distribution at the tissue–implant interface. The non-gradient composite PSU–CF 1D does not exhibit such a good biomimetic match. The Young's modulus of gradient composites is well-matched and does not distort the stress distribution in the segment C6–C7 of the cervical spine. Matching the materials with respect to Young's modulus values can minimize the risk of over-rigidness in intervertebral disc implants.
- The results of the *in vitro* tests conducted with a long-term static load displayed sufficient strength of materials V1, V2 and O3.
- On the basis of the obtained results, the material V1 was selected for the fatigue test. The fatigue tests performed proved this composite to be suitable for intervertebral disc implant, as it exhibited satisfactory parameters of fatigue strength.
- The biomimetic gradient composites constitute a very prospective group of biomaterials, mainly because of the possibility to control the gradient of Young's modulus, which assures the proper stress distribution at the implant–bone interface.

Acknowledgements

The Project has been financed from statutory research budget No. 11.11.160.616 of the AGH University of Science and Technology in Kraków.

References

[1] DOBLARE M., GARCIA J.M., GOMEZ M.J., *Modelling bone tissue fracture and healing: a review*, Eng. Fract. Mech., 2004, 71, 1809–1840.

[2] SNYDER B.D., HAYES W.C., *Multiaxial structure property relations in trabecular bone*, [in:] Mow V.C., Ratcliffe A., Woo S.L-Y. (eds.), *Biomechanics of Diarthrodial Joints*, Springer, New York 1990, 31–59.

[3] ADAMS M.A., HUTTON W.C., *The effect of posture on the fluid content of lumbar intervertebral disks*, Spine, 1983, 8, 665–671.

[4] WILDER D.G., POPE M.H., SEROUSSI R.E., DIMNET J., *Creep response of the statically and cyclically loaded lumbar motion segment*, Trans. Orthop. Res. Soc., 1987, 1, 367.

[5] MURUGAN R., RAMAKRISHNA S., *Development of nanocomposites for bone grafting*, Comp. Sci. Tech., 2005, 65, 2385–2406.

[6] CHŁOPEK J., MORAWSKA-CHOCHÓŁ A., BAJOR G., ADWENT M., CIEŚLIK-BIELECKA A., CIEŚLIK M., SABAT D., *The influence of carbon fibres on the resorption time and mechanical properties of the lactide–glycolide co-polymer*, J. Biomater. Sci. Polymer Edn., 2007, 18, 11, 1355–1368.

[7] PAVANATTI S.L., CARVALHO ZAVAGLIA C.A., BELANGERO W.D., KAWANO Y., *Study of biocompatibility of particles and rods of polysulfone*, Acta Ortop. Bras., 2001, 9, 3, 11–18.

[8] PN-EN ISO 14130:1997 *Material composites reinforced with fiber. Marking conventional interlaminar stress by short beam.*

[9] ZYSSET P.K., *A review of morphology-elasticity relationships in human trabecular bone: theories and experiments*, J. Biomech., 2003, 36, 1469–1485.

[10] YOGANANDAN N., KUMARESAN S., PINTAR A., *Biomechanics of the cervical spine.* Part 2. *Cervical spine soft tissue responses and biomechanical modeling*, Clin. Biomech., 2001, 16, 1–27.

[11] ADAMS M.A., STEFANAKIS M., DOLAN P., *Healing of a painful intervertebral disc should not be confused with reversing disc degeneration: Implicates for physical therapies for discogenic back pain*, Clin. Biomech., 2010, 25, 961–971.

[12] BĘDZIŃSKI R., *Biomechanika Inżynierska* (*Biomechanics Engineering*), ISBN 83-7085-240-8 Wrocław, 1997.

[13] SKRZYPIEC D.M., POLLINITE P., PRZYBYŁA A., DOLAN P., ADAMS M.A., *The internal mechanical properties of cervical intervertebral discs as revealed by stress profilometry*, Eur. Spine J., 2007, 16, 1701–1709.

[14] NICHOLSON P.H.F., CHENG X.G., LOWET G., BOONEN S., DAVIE M.W.J., DEQUEKER J., VAN DER PERRE G., *Structural and material mechanical properties of human vertebral cancellous bone*, Med. Eng. Phys., 1997, 19, 8, 729–737.

[15] CHOU T.W., *Structure and properties of composites*, 2005, 13/14, 98–99.

[16] KŁYSZ S., LISIECKI J., BĄKOWSKI T., *Modyfikacja równania do opisu krzywych Wöhlera (Equation modification to description of Wöhler curves) W*, Scientific Paper ITWL, 2010, 27, 93–97.

[17] CHŁOPEK J., *Composite materials for medicine*, Composites, 2001, 1, 50–54.

[18] HOJO Y., KOTANI Y., ITO M., ABUMI K., KADOSAWA T., SHIKINAMI Y., MINAMI A., *A biomechanical and histological evaluation of a bioresorbable lumbar interbody fusion cage*, Biomaterials, 2005, 26, 2643–2651.

[19] LEE C.K., GOEL V.K., *Artificial disc prosthesis: design concepts and criteria*, The Spine Journal, 2004, 4, 209S–218S.

[20] NOAILLY J., AMBROSIO L., TANNER K.E., PLANELL J.A., LACROIX D., *In silico evaluation of a new composite disc substitute with a L3–L5 lumbar spine finite element model*, Eur. Spine J., 2012, 21, S675–S687.

[21] HANSSON T.H., KELNER T.S., SPENGLER D.M., *Mechanical Behavior of the Human Lumbar Spine. II. Fatigue Strength During Dynamic Compressive Loading*, J. Orthopaed. Res., 1987, 5, 479–487.

[22] CHAFFIN D.B., ANDERSSON G.B.J., *Occupational biomechanic*, 1991, A Wiley-Interscience Publication.

[23] CHEUNG J.T.M., ZHANG M., CHOW D.H.K., *Biomechanical responses of the intervertebral joints to static and vibrational loading: a finite element study*, Clin. Biomech., 2003, 18, 790–799.

[24] TYLMAN D., *Patomechanika bocznych skrzywień kręgosłupa* (*Pathomorphology of lateral spine curvate*), Warszawa 1972.

[25] BORKOWSKI P., *Biomechanical analysis of artificial lumbar disc*, Bio-algorithms and Med-systems, 2005, 1, 1/2, 143–146.

[26] GZIK M., WOLAŃSKI W., TEJSZERSKA D., *Experimental determination of cervical spine mechanical properties*, Acta of Bioengineering and Biomechanics, 2008, 10, 4, 49–54.

[27] YAO J., TURTELTAUB S.R, DUCHEYNE P., *A three-dimensional nonlinear finite element analysis of the mechanical behavior of tissue engineered intervertebral discs under complex loads*, Biomaterials, 2006, 27, 377–387.

[28] IATRIDIS J.C., GWYNN I., Mechanisms for mechanical damage in the intervertebral disc annulus fibrosus, J. Biomech., 2004, 37, 1165–1175.